CrossMark

Carbon Dioxide Sequestration via Steelmaking Slag Carbonation in Alkali Solutions: Experimental Investigation and Process Evaluation

Chen-Ye Wang[1,2] · Wei-Jun Bao[2] · Zhan-Cheng Guo[1] · Hui-Quan Li[2]

Abstract

Carbon dioxide mineral sequestration with steelmaking slag is a promising method for reducing carbon dioxide in a large-scale setting. Existing calcium oxide or calcium hydroxide in steelmaking slag can be easily leached by water, and the formed calcium carbonate can be easily wrapped on the surface of unreacted steelmaking slag particles. Thus, further increase in the carbonation reaction rate can be prevented. Enhanced carbon dioxide mineral sequestration with steelmaking slag in dilute alkali solution was analysed in this study through experiments and process evaluation. Operating conditions, namely alkali concentration, reaction temperature and time, and liquid-to-solid ratio, were initially investigated. Then, the material and energy balance of the entire process was calculated, and the net carbon dioxide sequestration efficiency at different reaction times was evaluated. Results showed that dilute alkali solution participated in slowing down the leaching of active calcium in the steelmaking slag and in significantly improving carbonation conversion rate. The highest carbonation conversion rate of approximately 50% can be obtained at the optimal conditions of 20 g/L alkali concentration, 2 mL/L liquid-to-solid ratio, and 70 °C reaction temperature. Carbonation reaction time significantly influences the net carbon dioxide sequestration efficiency. According to calculation, carbon dioxide emission of 52.6 kg/t-slag was avoided at a relatively long time of 120 min.

Keywords Steelmaking slag · Dilute alkali solution · CO_2 mineral sequestration · Process evaluation

1 Introduction

With the increased use of fossil fuels in industries, large amounts of CO_2 are emitted to the atmosphere, which is widely recognized as one of the main causes of global warming. At present, a number of technologies, known as carbon capture and storage (CCS) technologies, are available to decrease CO_2 emissions from industries. There are three principal existing CCS approaches including geological storage, ocean storage, and mineral sequestration.

One of the three approaches, CO_2 mineral carbonation, is a CCS technology, in which CO_2 is stored in solid carbonate. This action provides potential advantages over other CCS technologies [1, 2]. The major advantages of sequestrating CO_2 by mineral carbonation include a final product that is known to be stable over geological time frames, a vast quantity of raw materials for binding CO_2 available across the globe, and the exothermic characteristic of the entire process. Natural minerals and industrial solid residua containing calcium or magnesium can be employed as raw materials for CO_2 mineral sequestration [3]. Compared with natural minerals, solid residue offers numerous advantages for use, including low cost, high reactivity, and fast reaction rate [4, 5]. The use of industrial solid residua for CO_2 mineral sequestration has been the focus of considerable attention in recent years because of the high calcium content.

Steelmaking slag is a typical industrial solid residue. The annual amount of steelmaking slag produced in China is estimated to be more than 50 Mt, and the accumulation of steelmaking slag has caused numerous environmental

✉ Hui-Quan Li
  hqli@ipe.ac.cn

1 State Key Laboratory of Advanced Metallurgy, University of Science and Technology Beijing, Beijing 100083, China

2 Key Laboratory of Green Process and Engineering, National Engineering Laboratory for Hydrometallurgical Cleaner Production Technology, Institute of Process Engineering, Chinese Academy of Sciences, Beijing 100190, China

problems, such as dust pollution, water pollution, and release of heavy metal elements into the environment. Steelmaking slag is usually composed of CaO, MgO, Al_2O_3, SiO_2, and other basic oxides. The high content of basic oxides indicates that steelmaking slag possesses a high alkalinity and a high total theoretical CO_2 sequestration capacity, which has been evaluated at approximately 0.25 kg CO_2/1 kg slag based on the total calcium content [6]. Therefore, the use of steelmaking slag for CO_2 mineral sequestration is a promising method because of the high calcium oxide content.

CO_2 mineral sequestration with steelmaking slag can be classified as a direct route when the basic oxides are carbonated in a single step or as an indirect route when the reactive components are first extracted from the steelmaking slag by using a recycling medium, and then by carbonation in a separate step [6–8]. The development of extracted media performs a key function in indirect CO_2 mineral sequestration, which should exhibit high activity for leaching out reactive components from steelmaking slag and should be easily recovered via the carbonation step [9, 10]. With the possible complication of indirect CO_2 mineral sequestration in the operating procedure, the energy consumption of high-value carbonate production is increased. Direct routes have been extensively investigated with the advantage of a simple process and implemented by using direct gas–solid carbonation (dry route) or direct aqueous carbonation reaction route (wet route). Yu and Wang [11] investigated the carbonation characteristics of steel slag for CO_2 sequestration in the dry route and determined that, under the high reaction temperature condition (> 500 °C), the steelmaking slag exhibit better CO_2 sequestration when CO_2 concentrations are lower than 20% or higher than 75%. Tian et al. [12] investigated the direct gas–solid carbonation of steelmaking slag in the presence of SO_2 at typical flue gas concentrations. The existence of $Ca(OH)_2$ in the steelmaking slag could be carbonated with a fast reaction rate, and the obtained maximum CO_2 sequestration was 88.5 kg/t-slag in a typical flue at 600 °C. Thus, we can conclude that a high-temperature condition is highly demanded for accelerating the carbonation reaction in this direct dry route, thereby restricting the application.

As a result of the dissolution of CO_2 in water to form carbonic acid and the use of steelmaking slag that contains active calcium and magnesium components, the wet route becomes relatively easy to conduct. Huijgen et al. [13–15] systematically investigated the direct wet carbonation process with steelmaking slag as raw material. Under optimum conditions of 200 °C reaction temperature, 20 bar CO_2 pressure, 2 kg/kg liquid-to-solid (L/S) ratio, and < 38 μm particle size, the obtained carbonation conversion rate was as high as 67%. Based on the simulation process conducted by using the Aspen Plus software, the energy consumption of the entire process includes power of 400 kW h and heat of 354 kWh/1 t CO_2 sequestered, and the total sequestration cost is evaluated to be as high as 64 €/t CO_2 sequestered. Stolaroff et al. [16] proposed a new process for CO_2 mineral sequestration with steelmaking slag in the atmosphere to decrease energy consumption. The process mainly involves the calcium-saturated solution, which was initially obtained from steelmaking slag leached by water and sprayed onto the surface of the piled steelmaking slag. This process exhibits low energy consumption, and the operating cost is estimated to be US $8/t CO_2 sequestered. However, a large space is necessary for piling steelmaking slag in this new process, and a low CO_2 sequestration efficiency results from a low content of CaO or $Ca(OH)_2$ in the steelmaking slag.

The formed calcium carbonate can also be easily wrapped on the surface of unreacted steelmaking slag particles, thereby preventing further increase in carbonation reaction rate. Numerous studies have focused on the efficiency of a carbonation reactor for enhancing CO_2 mineral sequestration with steelmaking slag. Chang et al. [17] conducted a performance evaluation of the carbonation of steelmaking slag in a slurry reactor. The highest carbonation conversion rate obtained is approximately 72% at a reaction time of 1 h, an operating pressure of 101 kPa, and a temperature of 60 °C. Pan et al. [18–20] investigated the accelerated carbonation of steelmaking slag coupled with metalworking wastewater in a rotating packed bed and high-gravity rotating packed bed reactor. Results showed that the applied rotating packed bed or high-gravity rotating packed bed reactor can improve the mass transfer rate among phases owing to its high centrifugal force and excellent micromixing ability, thereby achieving a superior CO_2 fixation efficiency. In addition, life-cycle assessment for the high-gravity carbonation process shows a net CO_2 sequestration amount of 1279 kg CO_2-eq/t basic furnace slag, with the carbonated slag utilized as cement substitution material. Furthermore, Santos et al. [21] reported an enhanced steelmaking slag mineral carbonation in an ultrasound reactor. Passivation layers surrounding the unreacted particle core can be removed by ultrasound, possibly reducing mass transfer inhibition and increasing carbonation conversion rate. We proposed a new process of enhanced steelmaking carbonation in dilute alkali solution to alleviate the wrapping of formed calcium carbonate on the surface of unreacted particle core. Aragonite could be generated at certain temperature and alkali condition, which would cause difficulties in wrapping of the unreacted particle core. In this study, alkali concentration, reaction temperature and time, and L/S ratio are initially investigated, and then the material and energy balance of the entire process was

calculated, and the net CO_2 sequestration efficiency at different reaction times was further evaluated.

2 Experimental Section

2.1 Raw Materials

The steelmaking slag used in this study was converter slag obtained from Shougang Qian'an Iron and Steel Co. Ltd., China. The particle size of the steelmaking slag used was less than 75 μm. The chemical composition and crystal form of the used steelmaking slag were analysed by using X-ray fluorescence (XRF) and X-ray diffraction (XRD), respectively. In Table 1, the total content of calcium and magnesium in steelmaking slag was approximately 52.04%, which indicated that the theoretically sequestrated CO_2 per ton steelmaking slag could be calculated as 439.8 kg. Combined with XRD analysis, as shown in Fig. 1, the existence of calcium oxide, calcium carbonate and tricalcium silicate could be confirmed. In the experiments, all chemicals used were of analytical grade and deionised water was used.

2.2 Experimental Procedure

The experiments were conducted in a 2-L four-mouth flask with a temperature monitor and gas flow meter. The schematic diagram of the apparatus used in this work is illustrated in Fig. 2. An automatic proportional, integral, and derivative control system managed the heating rate, agitation, and temperature of the flask. The dilute alkali solution and steelmaking slag were added into the flask, and then CO_2 was piped into the system. The mixture was then digested at a certain temperature at different residence times. After the reaction, the carbonated slag was filtered and washed with deionised water. The effects of alkali concentration, reaction temperature and time, L/S on steelmaking slag carbonation conversion rate were investigated according to designed experiments.

The composition of the initially used steelmaking slag was analysed using X-ray diffraction (XRD) (X'Pert Pro MPD X-ray diffractometer from PANalytical) and X-ray fluorescence spectroscopy (XRF) (SHIMADZU Lab Center XRF-1700, Japan). The content of carbon in the carbonated

Table 1 Composition of steelmaking slag analysed by XRF (in oxide) (wt%)

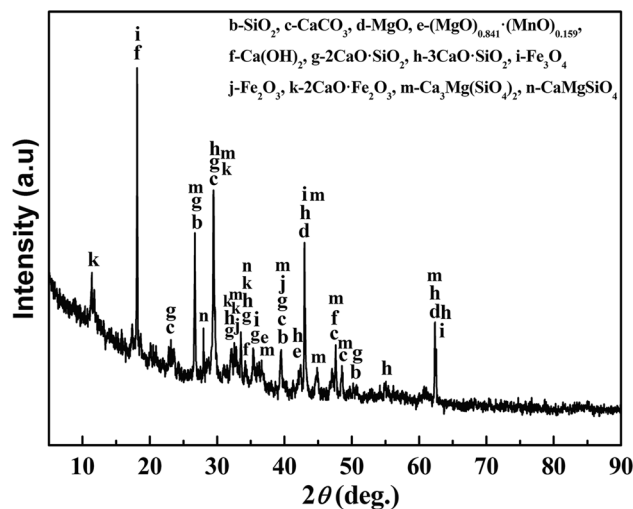| CaO	SiO₂	Al₂O₃	Fe₂O₃	MgO	P₂O₅	BaO	MnO
42.21	19.62	5.93	16.59	9.83	0.76	0.12	1.18

Fig. 1 XRD pattern of the raw steelmaking slag

slag was analysed with carbon–sulphur determinator (LECO, CS-344, USA). The crystal phase and morphology of the carbonated slag was analysed using XRD and SEM (JSM 6700F NT, Japan), respectively. The chemical components of the leaching liquor were analysed by using ICP-OES (Optimal 5300DV of PerkinElmer instruments, 1300 W, carrier gas flow 0.08 L/min, peristaltic pump flow 1.5 L/min).

The carbonation conversion rate of steelmaking slag during the experiment was calculated as follows:

$$x = \frac{44 \times m_1}{12 - 44 \times m_1} \times \frac{1000}{439.8} \times 100\%, \tag{1}$$

where x is the carbonation conversion rate, %; m_1 is the carbon content in the carbonated slag, %; 44 is the relative molecular mass of CO_2, g/mol; 12 is the relative molecular mass of carbon, g/mol; 439.8 is the binding amount of CO_2 by steelmaking slag per ton in theory, kg/t-slag. Notably, with the low content of carbon (0.81%) in the initially used steelmaking, the calculated carbonation conversion rate presents a slight deviation to disregard this influence.

3 Results and Discussion

3.1 Experimental Investigation

As studied by a previous researcher, the process of carbonation steelmaking slag in aqueous solution mainly involves three sub-processes, including the CO_2 diffusion, dissolution, and ionization sub-process, active calcium dissolution and ionization sub-process, and the calcium carbonate precipitation sub-process [6, 17]. With the addition of alkali to the aqueous solution for the new process of enhanced steelmaking slag carbonation, the
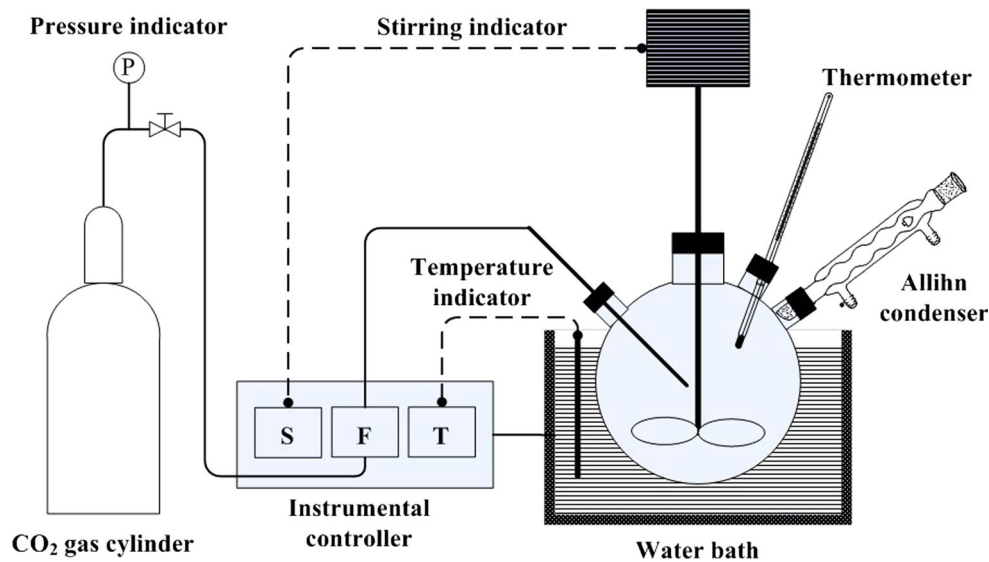
Fig. 2 Schematic diagram of experimental set-up for this enhanced carbonation of steelmaking slag

alkali performs an evident function of enhancing CO_2 absorption. Meanwhile, the dissolution and ionization of active calcium may become difficult in alkali solution, thus influencing the carbonation conversion rate of steelmaking slag. Therefore, the effects of alkali concentration, reaction temperature and time, and L/S on steelmaking slag carbonation have been experimentally investigated for obtaining the optimal conditions.

3.1.1 Effect of Alkali Concentration

Figure 3 shows the variation of carbonation conversion of steelmaking slag with reaction time at various alkali concentrations, while other parameters were kept constant
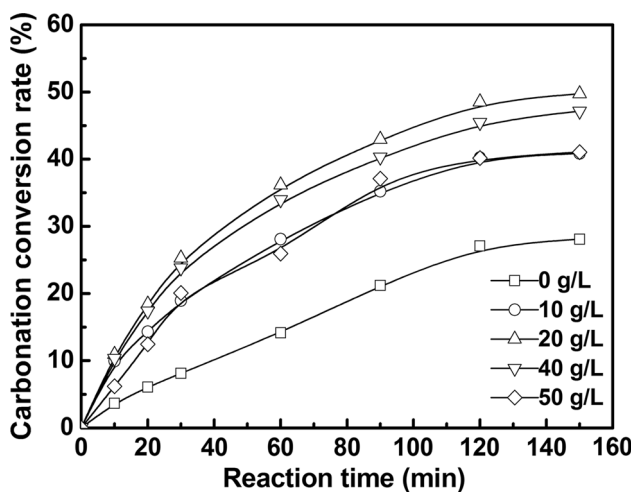

Fig. 3 Effect of the NaOH concentration on the carbonation conversion rate of steelmaking slag under the conditions of reaction temperature 70 °C, L/S 2 mL/g)

(reaction temperature, 70 °C; S/L ratio, 2 mL/g). As could be seen from Fig. 3, carbonation conversion rate increased with time at various alkali concentrations. When in water system, that is, alkali concentrations of 0 g/L, carbonation conversion rate gradually increased with reaction time, and the obtained highest value was 27.1% at 120 min, whereas the growth rate of carbonation conversion rate decreased with the increase in time when in an alkali system. As could be seen from Fig. 3, carbonation conversion rate first increased rapidly as alkali concentration increased from 0 to 20 g/L and decreased from 40 to 50 g/L at varied reaction time. At an alkali concentration of below 20 g/L, the increase in alkali solution could considerably improve carbonation conversion rate, whereas carbonation conversion rate decreased with further increase in alkali concentration. At an alkali concentration of 20 g/L, carbonation conversion rate reached the maximum, which was about two times that of the water system. Therefore, the optimum concentration of alkali was selected as 20 g/L.

To investigate the mechanism of the effects of different alkali concentrations on the carbonation conversion rate of steelmaking slag, we detected the contents of calcium and silicon in the leaching solution after carbonation at varied reaction times. As shown in Fig. 4a, we could see that, with the increase in reaction time, the amount of calcium in the leaching solution increased to a maximum and then decreased to a minimum, while the maximum leaching amount of calcium first decreased sharply and then increased with the alkali concentration. At an alkali concentration of 0 g/L or as high as 50 g/L, the largest amount of calcium was leached in solution at the reaction time of approximately 30 or 60 min, and low maximum leaching amount of calcium was displayed at the reaction time of
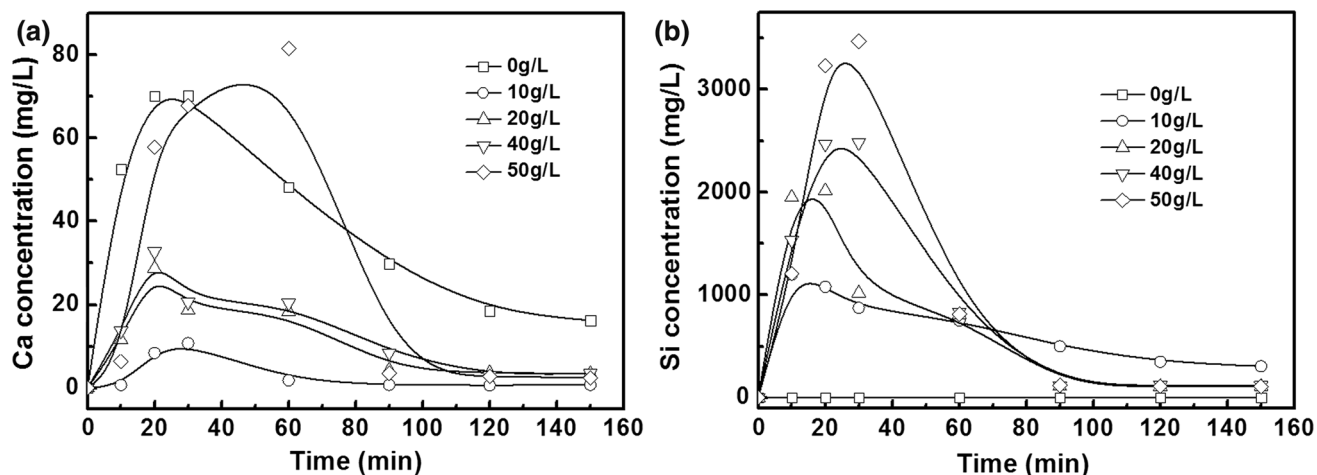
Fig. 4 Effect of the NaOH concentration on the leaching of Ca (**a**) and Si (**b**) under the conditions of reaction temperature 70 °C, *L/S* 2 mL/g

approximately 20 min at an alkali concentration between 10 and 40 g/L. As seen in Fig. 4b, in a similar response as calcium, the amount of silicon in leaching solution increased to a maximum and then decreased to a minimum with the increase in reaction time at an alkali concentration exceeding 0 g/L, whereas leached silicon could not be detected in water system only. However, different from calcium leaching, the maximum leaching amount of silicon continually increased with alkali concentration. When a large amount of calcium was leached in aqueous solution, the degree of $CaCO_3$ supersaturation increased and improved the crystallization rate of $CaCO_3$ simultaneously. Thus, the formed $CaCO_3$ easily wrapped on the surface of the unreacted particle core, resulting in difficulty in improving carbonation conversion rate. In addition, a certain portion of the calcium silicate phase in steelmaking slag could react with dilute alkali and release more calcium ions and silicate, thus increasing the active component for the reaction with CO_2. However, the presence of a large number of calcium ions could lead to the easy wrapping of the formed $CaCO_3$ on the surface of the unreacted particle core. By combining the results shown in Figs. 3 and 4, we could conclude that, when alkali concentration was lower than 20 g/L, the existence of alkali could effectively inhibit the dissolution and ionization of active calcium from steelmaking slag. Furthermore, the leached calcium remained in the low concentration range, thereby reducing the occurrence of formed $CaCO_3$ wrapped on the surface of the unreacted particle core, thereby increasing steelmaking slag carbonation conversion rate. In addition, when the alkali concentration exceeds 20 g/L and with greater dissolution of calcium silicate phase in steelmaking slag, the higher amount of released calcium ions could improve formed $CaCO_3$ wrapping on the surface of the unreacted particle core. This wrapping seriously hinders the

carbonation reaction of steelmaking slag, resulting in the decrease in carbonation conversion rate.

3.1.2 Effect of Reaction Temperature and Time

Figure 5 shows the variation in carbonation conversion rate of the steelmaking slag with reaction time at different reaction temperatures, whereas other parameters were kept constant (alkali concentration, 20 g/L; *S/L* ratio, 2 mL/g). As could be seen from Fig. 5, carbonation conversion rate increased with time at various reaction temperatures. When the reaction temperature is as low as 40 °C, carbonation conversion rate increased rapidly with the increase in reaction time to 60 min. Afterwards, only 4% increment of carbonation conversion rate could be detected for another 60 min, meaning that the carbonation reaction could almost reach equilibrium at 60 min at the reaction
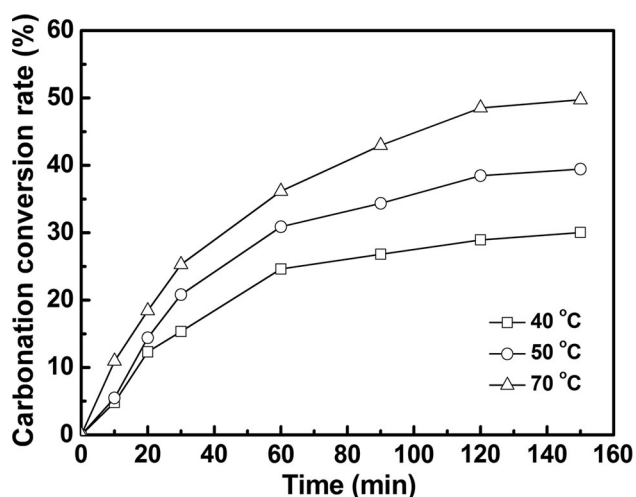

Fig. 5 Effect of the reaction temperature on the carbonation conversion rate of steelmaking slag under the conditions of NaOH concentration 20 g/L, *L/S* 2 mL/g

temperature of 40 °C. However, when the reaction temperature reaches a high level of 70 °C, the carbonation conversion rate continually increased rapidly with reaction time, and approximately 12% increment of carbonation conversion rate could be detected for the last 60 min. This finding indicates that the equilibrium time for this enhanced carbonation requires a minimum of 120 min. This result was considerably different from that in the water system, as studied by a previous researcher [17] because of the complex reactions, which include the absorption of CO_2 gas, the dissolution of a certain part of the calcium silicate phase in alkali solution, and the precipitation of $CaCO_3$. As carbonation reactions usually occur at atmospheric pressure and the increased temperature does not favour CO_2 absorption, higher temperature was not investigated. Thus, the experiments were performed at 70 °C.

For further study of the influence of reaction temperature on the carbonation conversion rate of steelmaking slag, characterization and analysis of the carbonated slag after 120 min was conducted by X-ray diffraction (XRD) and scanning electron microscopy (SEM). As shown in Fig. 6, only the $CaCO_3$ crystal type of calcite could be detected in the carbonated slag for the reaction temperature of 40 and 50 °C. Two types of the $CaCO_3$ crystal, namely calcite and aragonite, could be detected when the temperature was further increased to 70 °C. Thus, the $CaCO_3$ crystal type of aragonite could be formed only at a high reaction temperature of 70 °C for the enhanced carbonation process. Figure 7 shows that the raw steelmaking slag was composed of different sizes of randomly accumulated particles.
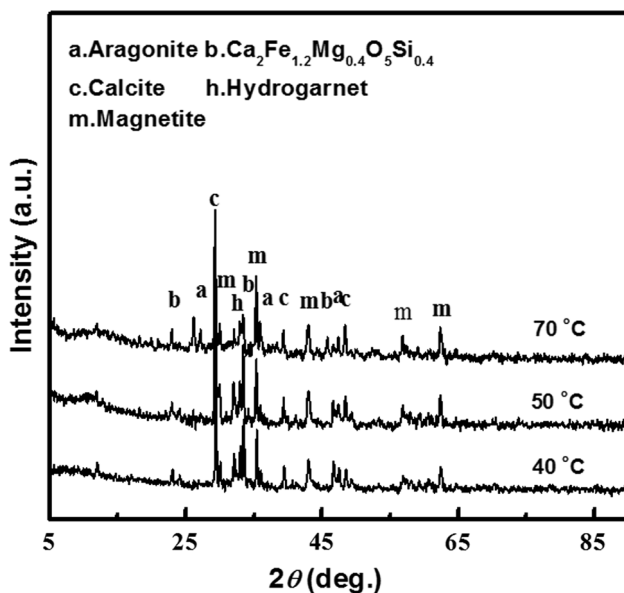

Fig. 6 XRD patterns of carbonated slag at different reaction temperature under the conditions of NaOH concentration 20 g/L, L/S 2 mL/g, reaction time 120 min

Moreover, the surface of the slag was not neat and possessed a small hole. When the reaction temperatures were 40 and 50 °C, the obtained carbonated slag was composed of irregular solid particles, which contained larger particles with exposed smooth surfaces, whereas the rest of the smaller particles were covered by other fine particles. When the reaction temperature further increased to 70 °C, the obtained carbonated slag was composed of coarse solid particles with a smooth surface, long rod-like particles, and certain small round particles. By combining Figs. 6 and 7, we could identify that the coarse solid particles with smooth surface were attributed to the calcite $CaCO_3$ crystal type, the long rod-like particles were attributed to the aragonite $CaCO_3$ crystal type, and the leftover small round particles may be attributed to silicon-containing precipitate. In addition, the formed aragonite particles formed minimal attachment to other particles, while the formed calcite particles usually displayed aggregation with other particles. This observation further confirmed that the formed aragonite would not wrap on the surface of the unreacted particle core. Therefore, we conclude that the surface of the unreacted particle core is difficult to be wrapped by formed aragonite particles, and an appropriate increase in reaction temperature favours the formation of more aragonite particles, thus further improving the carbonation conversion rate.

3.1.3 Effect of Liquid-to-Solid Ratio

For obtaining the optimal conditions, the effect of the L/S on the carbonation conversion rate was studied at the reaction temperature of 70 °C and alkali concentration of 20 g/L. As could be seen from Fig. 8, carbonation conversion rate increased with time at various L/S ratios, whereas the growth rate of carbonation conversion rate decreased with the increase in L/S ratio. When the L/S ratio does not exceed 2 mL/g, carbonation conversion rate continually increased with reaction time, and a considerably evident increment of carbonation conversion rate could be found, indicating that carbonation reaction did not reach equilibrium even with a long reaction time of 120 min. When the L/S exceeded 2 mL/g, the increment of carbonation conversion rate could be hardly detected at the reaction time of 60 min with an L/S of 4 mL/g and 30 min with the L/S of 8 mL/g. We could conclude that L/S considerably influences the time of carbonation reactions to reach equilibrium, and the higher L/S may induce the carbonation reaction to reach equilibrium at an earlier time. Notably, when the reaction time was shorter than 60 min, the carbonation conversion rate increased to the highest value, with the L/S increasing to 4 mL/g. In contrast, when the reaction time was longer than 60 min, the highest carbonation conversion rate could be obtained at the L/S of
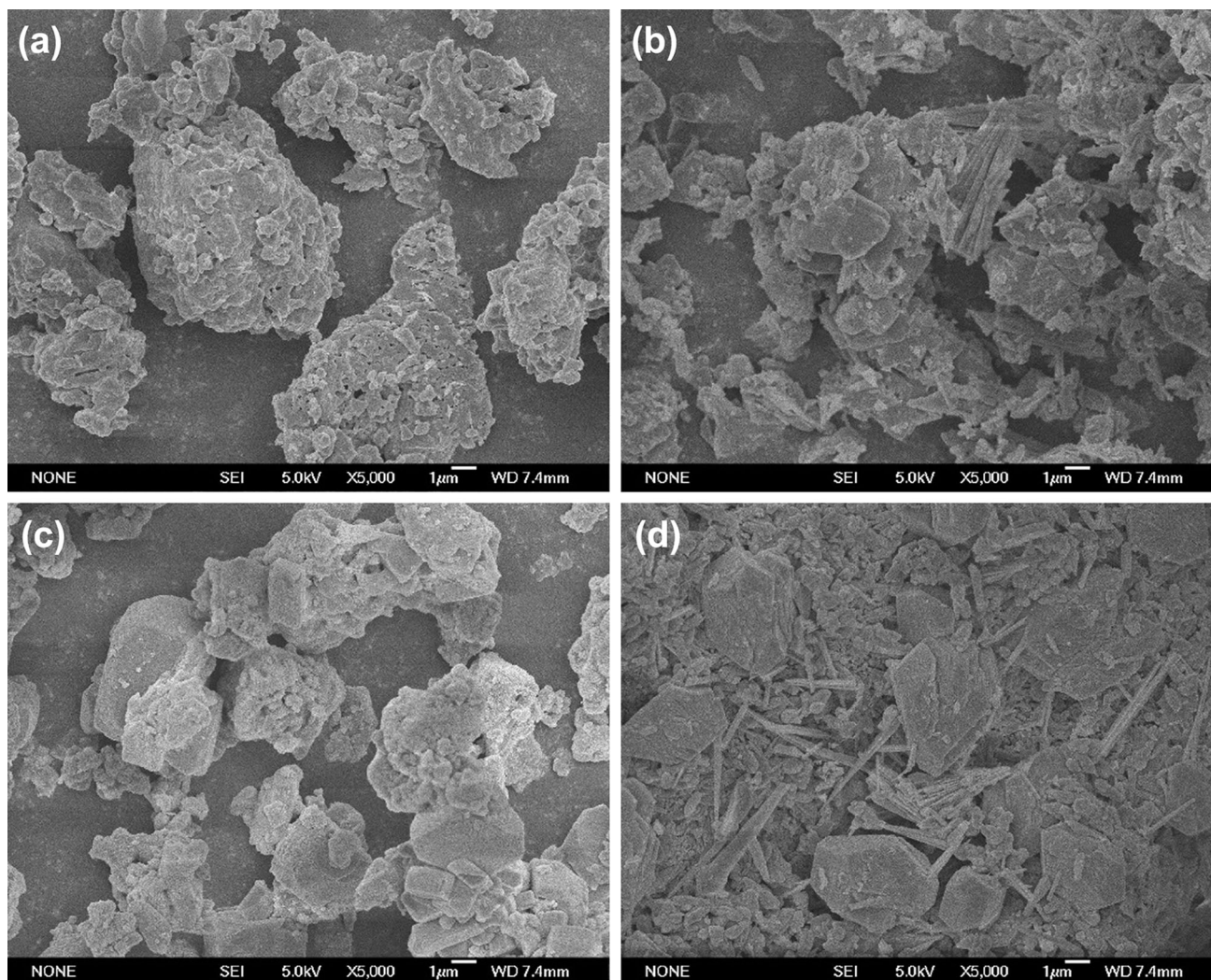
Fig. 7 SEM photographs of the raw steelmaking slag and carbonated slag produced at different react temperature under the conditions of NaOH concentration 20 g/L, L/S 2 mL/g, reaction time 120 min: **a** raw material; **b** 40 °C; **c** 50 °C; **d** 70 °C

2 mL/g. When the L/S was as high as 8 mL/g, the obtained carbonation conversion rate after 30 min reaction time was considerably lower than the values obtained at the L/S of 2 and 4 mL/g. These results indicate that high L/S opposes carbonation conversion rate improvement for enhancing carbonation process possibility because the dissolution of calcium silicate increased with L/S and released more calcium ions to the aqueous solution. Thus, the wrapping of the formed $CaCO_3$ on the surface of the unreacted particle core increased. To obtain high carbonation conversion rate and decrease alkali solution recycling, we should select the optimal L/S ratio of 2 mL/g.

3.2 Process Evaluation

3.2.1 Mass Balance Calculation

The entire process of the enhanced CO_2 mineral carbonation with steelmaking slag in dilute alkali solution is shown in Fig. 9. The process steps include grinding, premixing, carbonation, filtering and washing, and drying. For full-scale application of this process, a vertical mill was used for grinding, two stirred tank reactors were used for premixing and carbonation, a vacuum belt filler was used for filtering and washing, and combined double-paddle driers and tray driers were used for drying. Both single-stage centrifugal pumps and belt conveyors were used for liquid and slurry transportation and for bulk particle transportation. Given the reaction of CO_2 with dilute alkali during the carbonation process to produce $NaHCO_3$, which
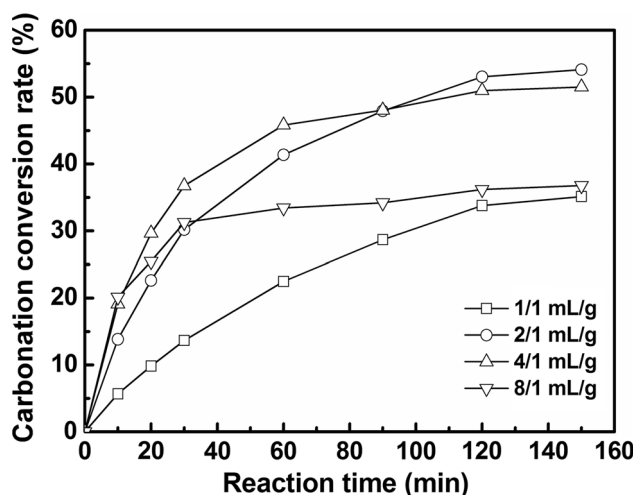
Fig. 8 Effect of the liquid-to-solid ratio on the carbonation conversion of steelmaking slag under the conditions of reaction temperature 70 °C, NaOH concentration 20 g/L

Table 2 Mass balance of the overall process

Materials flow	Carbonation reaction time (min)		
	30	60	120
Input			
Steelmaking slag (t/h)	56.31	39.31	29.34
Dilute alkali solution (m³/h)	112.6	78.6	58.7
CO₂ gas (t/h)	6.25	6.25	6.25
Added water (kg/h)	15.64	11.39	8.90
Added alkali (kg/h)	125.1	91.1	71.2
Output			
Carbonated residue (kg/h)	62.56	45.56	35.59

can react with free calcium and magnesium to regenerate dilute alkali, dilute alkali circulation can be achieved.

The aforementioned experiments resulted in the following optimum conditions for CO_2 mineral carbonation with steelmaking slag: NaOH concentration, 20 g/L; reaction temperature, 70 °C, and L/S ratio, 2 mL/g. Under optimum conditions, 1 t of steelmaking slag is consumed to bind 111 kg CO_2 in 30 min, 159 kg CO_2 in 60 min, and 213 kg CO_2 in 120 min. Assuming that 50,000 t CO_2 is directly sequestrated by steelmaking slag per year, the annual working time is 8000 h, and the amount of CO_2 sequestrated is 6.25 t/h. Therefore, the required amounts of steelmaking slags are 56.31, 39.31, and 29.34 t/h with the reaction times of 30, 60, and 90 min, respectively. Simultaneously, the volume flow rates of the dilute alkali

solution were 112.6, 78.6, or 58.7 m³/h, and the mass flow rates of carbonated slag are 62.56, 45.56, or 35.59 t/h at different reaction times. Given the easy adherence of dilute alkali onto the surface of carbonated slag, we estimated that the moisture content of the filter cake was 20%, and the NaOH concentration in the final obtained washing solution is 8 g/L. Approximately 125.1, 91.1, or 71.2 kg/h NaOH and 15.64, 11.39, or 8.90 t/h fresh water should be added during filtering and washing process at different reaction times. Based on the aforementioned calculations, the results of the mass balance of the entire process are listed in Table 2. Notably, the adherence of dilute alkali and the moisture in carbonated slag would induce a decrease in circulation of dilute alkali solution. Thus, NaOH and fresh water should be added. Moreover, the added fresh water can be used for washing the carbonated slag first and then combined with filtered dilute alkali solution for recycling, displaying the advantage of partial NaOH recovery from the filter cake of the carbonated slag.
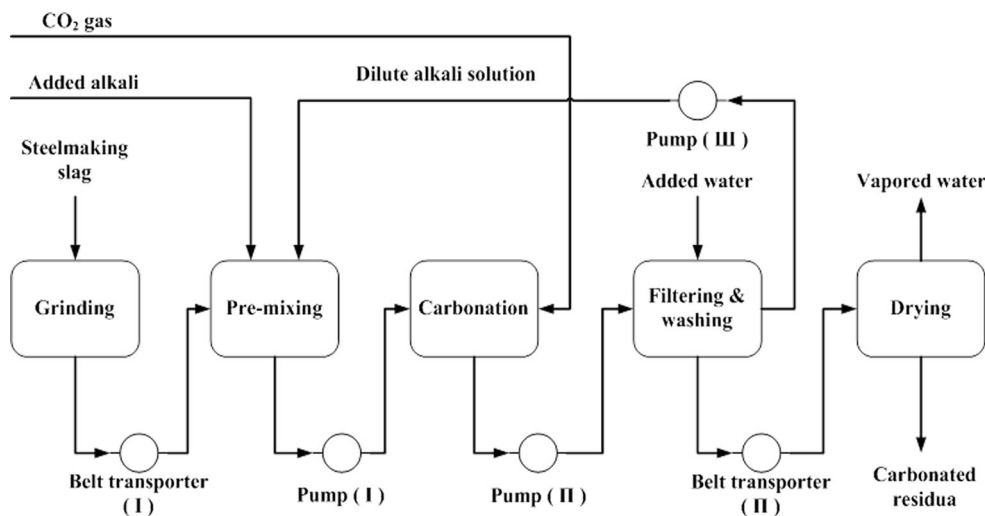

Fig. 9 Block diagram of the whole carbonation process with recyclable dilute alkali solution

3.2.2 Energy Consumption

The energy consumption of the entire process mainly includes power consumption during grinding, premixing, carbonation, filtering and washing, drying, CO_2 separation from flue gas, and material transport process, and steam consumptions during material heating, and CO_2 separation from flue gas process. However, CO_2 could be absorbed directly by using dilute alkali solution. Thus, CO_2 separation consumption can be ignored.

The grain size of steelmaking slag after cooling and iron recovery is normally 10 mm [22], which is larger than the required 75 μm. Thus, the grinding process is necessary. Usually, the grinded steelmaking slag with a specific surface area that exceeded 450 m^2/kg was preferred to utilization as steel slag cement. Therefore, a grain size of 75 μm for the grinded steelmaking slag is optimally selected in this work. Energy consumption during grinding process can be calculated by using the following empirical formula calculation:

$$W = 0.01 \times W_i \times \left(\frac{1}{\sqrt{d_1}} - \frac{1}{\sqrt{d_0}} \right), \tag{2}$$

where W_i is the Bond power index, d_0 is the grain size of steelmaking slag before grinding, and d_1 is the grain size of steelmaking slag after grinding. Given that the steel slag after magnetic separation is used as raw material and a vertical mill has now been successfully used for steelmaking slag grinding, W_i was set as 26.47 kW h/t [23]. The resulting energy consumption was 29.73 kW h/t-slag.

Equipment size should be determined to calculate power consumption during premixing and carbonation. According to the steelmaking slag grain density of 2600 kg/m^3 and the effective volume of the equipment of 2/3, stirring tank volumes were 100.7, 70.3, or 52.5 m^3 when the reaction time of the premixing process was set as 30 min. In addition, the carbonated stirring tank volumes were 100.7, 140.6, or 209.9 m^3 when the carbonation reaction times were 30, 60, or 120 min. Based on the research of Mattila and Zevenhoven [24], a cylindrical stirred reactor with a height/diameter ratio of 2 was used. The stirring tank diameters are 3.2, 3.6, 4.0, 4.5, or 5.1 m, with total volumes of 52.5, 70.3, 100.7, 140.6, and 209.9 m^3, respectively. The power consumption of the stirring tank can be calculated as follows:

$$P_{\text{stirring}} = N_p \times \rho \times n^3 \times d^5, \tag{3}$$

$$Re_v = \frac{\rho \times n \times d^2}{\eta}, \tag{4}$$

where P_{stirring} is the stirring power, N_p is the power factor, ρ is the density of the media, n is the speed of the agitator, d is the impeller diameter, Re_v is the Reynolds number, and

η is the viscosity of the media. For L/S ratio of 2 mL/g, the density of the media was 1258 kg/m^3 and the viscosity of the media was 1.0 mPa s. With the stirring speed of 160 rpm (2.67 s^{-1}) used in the industry, the diameter ratio of the impeller to stirring tank ranged from 0.21 to 0.7. In this study, the diameter ratio of the impeller to stirring tank was set as 0.35 to achieve complete mixing of the steelmaking slag and dilute alkali, thereby reducing power consumption during mixing. Besides, a stirring speed of 160 rpm is selected for the relative small stirring tank with a volume of 52.5 m^3, whereas the stirring speed for other larger stirring tanks was determined based on the constant flow state for the scale amplification of the stirring tank, which can be calculated as follows [25]:

$$n_i = n \times \left(\frac{V}{V_i} \right)^{1/3}, \tag{5}$$

where n_i is the stirring speed for amplified stirring tank, and V_i is the volume of amplified stirring tank. The stirring tank contained a double impeller and was equipped with three baffles. Thus, N_p was set as 0.96 [27]. Based on these settings, the calculation results of the stirring power during premixing and carbonation are listed in Table 3.

The lowest power consumption of a single-stage centrifugal pump can be calculated as follows [26]:

$$P_{\text{pump}} = \frac{G \times H \times m}{3600 \times \eta_{\text{efficiency}}}, \tag{6}$$

where P_{pump} is the pump power, G is the acceleration of gravity, H is the lift, m is the mass flow, and $\eta_{\text{efficiency}}$ is the efficiency factor for pump. The lowest power consumption of the belt conveyor can be calculated as follows [27]:

$$P_{\text{conveyor}} = 0.0006 \times m \times L + 0.0032 \times m \times H_c + 1.5, \tag{7}$$

where P_{conveyor} is the conveyor power, L is the length of the belt conveyor, and H_c is the hoisting height. For the pumps used in this process, H and η were set as 20 m and 0.6, respectively. For the belt conveyor, L and H_c were set as 20 and 5 m, respectively. Based on these settings, the calculation results of the power consumption of the conveying equipment are listed in Table 4.

The mixed slurry obtained after carbonation should be filtered and washed by using a horizontal vacuum belt filter. The filtration area for vacuum belt filter can be determined by its productive capacity of 1000 kg/(m^2 h) filter cake, which was estimated from the vacuum belt filter applied in wet phosphoric acid [28]. Thus, the needed filtration area can be calculated as 78.2, 57.0, and 44.5 m^2 with the carbonation reaction times of 30, 60, or 120 min, respectively. Accordingly, the installed powers for belt filter were selected as 30, 22, and 22 kW, and the needed

Table 3 Stirring power for premixing and carbonation process

Process	Stirring tank	Carbonation reaction time (min)		
		30	60	90
Premixing	Volume (m^3)	100.7	70.3	52.5
	Width (m)	4	3.6	3.2
	Height (m)	8	7.2	6.4
	Impeller diameter (m)	1.4	1.26	1.12
	Stirring speed (s^{-1})	2.15	2.42	2.67
	Stirring power (kW)	64.6	54.4	40.5
Carbonation	Volume (m^3)	100.7	140.6	209.9
	Width (m)	4	4.5	5.1
	Height (m)	8	9	10.2
	Impeller diameter (m)	1.4	1.58	1.78
	Stirring speed (s^{-1})	2.15	1.92	1.68
	Stirring power (kW)	64.6	83.1	103.8

Table 4 Power consumption of the transport equipment

Transporter	Power	Carbonation reaction time (min)		
		30	60	90
Belt conveyor (I)	Mass flow (t/h)	56.3	39.3	29.3
	Power consumption (kW)	3.1	2.61	2.31
Belt conveyor (II)	Mass flow (t/h)	62.6	45.6	35.6
	Power consumption (kW)	3.2	2.8	2.5
Pump (I)	Mass flow (t/h)	171.3	119.5	89.2
	Power consumption (kW)	15.5	10.8	8.1
Pump (II)	Mass flow (t/h)	177.4	125.7	95.4
	Power consumption (kW)	16.1	11.41	8.7
Pump (III)	Mass flow (t/h)	114.9	80.2	59.8
	Power consumption (kW)	10.4	7.3	5.4

power values for vacuum pumps, which were connected with belt filters, were 110, 110, and 90 kW, as shown in Table 5. The energy consumption of different drying methods also varies. Normally, the thermal efficiency of conduction drying is 85%, whereas that of convection drying was 30–60% [26]. In order to decrease the energy consumption of drying, combined double-paddle driers and disc driers were needed to dry the filter cake obtained after filtering and washing. The moisture content of the filter cake firstly increased to 10% in double-paddle driers and

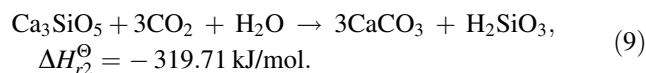**Table 5** Power consumption of the filtering and drying process

Process	Equipment	Carbonation reaction time (min)		
		30	60	90
Filtering	Filter cake (t/h)	78.2	57.0	44.5
	Filtration area (m^2)	78.2	57.0	44.5
	Power for belt filters (kW)	30	22	22
	Power for vacuum pumps (kW)	110	110	90
Drying	Water removed by paddle drier (t/h)	8.69	6.33	4.94
	Dry area for paddle drier (m^2)	728	523	414
	Power for paddle drier (kW)	546	397	310
	Water removed by disc drier (kg/h)	6.95	5.06	3.96
	Dry area for disc drier (m^2)	810	590	461
	Power for disc drier (kW)	135	98	77

then continually decreased to less than 0.1% in tray driers. We can calculate that the amounts of water removed by paddle driers are 8.69, 6.33, and 4.94 t/h, whereas those removed by disc driers were 6.95, 5.06, and 3.96 t/h at different reaction times. Furthermore, with the heat transfer temperature difference of 116.2 and 79.2 °C and heat transfer coefficients of 350 and 250 kJ/m^2 h for paddle driers and disc driers, respectively, the needed dry area for paddle driers are 728, 523, and 414 m^2, whereas those of disc driers are 810, 590 and 461 m^2. Based on the assumption that the installed power was 75 kW for the double-paddle drier with the drying area of 100 m^2 and with a drying area of 108 m^2, the installed power was 18 kW for the disc drier. The power consumption of the drying process can be calculated as also shown in Table 5.

Therefore, according to the aforementioned calculations, the power consumption of the integral process is listed in Table 6. As can be seen in the figure, power consumption markedly decreases with the increase in reaction time. Power consumed during grinding accounts for more than half of the power consumption of the entire process. With the consideration of carbonated slag utilized as cement substitution material, drying for carbonated slag is employed, but relatively high power consumption is required. Notably, with a long reaction time of 120 min, power consumption for the whole process decreases to as low as 246.8 kW h/t CO_2, which is considerably lower than the criteria suggested by the U.S. Department of Energy, that is, a cost-effective CO_2 capture facility should achieve a maximal energy consumption of 420 kW h/t CO_2 [29].

The steelmaking slag and dilute alkali solution were all heated from 20 to 70 °C, and the heat of carbonation should be further considered. Carbonation reaction heat mainly involves CO_2 reacting with calcium oxide and calcium silicates. For simplifying the calculation of reaction heat, only the carbonation reactions with calcium oxide and tricalcium silicate are calculated as follows:

$$CaO + CO_2 \rightarrow CaCO_3, \quad \Delta H_{r1}^{\Theta} = -177.76 \text{ kJ/mol}, \quad (8)$$

$$Ca_3SiO_5 + 3CO_2 + H_2O \rightarrow 3CaCO_3 + H_2SiO_3, \\ \Delta H_{r2}^{\Theta} = -319.71 \text{ kJ/mol}. \quad (9)$$

Therefore, the total heat consumption of the carbonation process can be calculated as follows:

$$Q = \left(\sum m_i \times c_{pi} \right) \times \Delta T_i - \frac{m_{slag} \times w_{CaO}}{56} \\ \times \Delta H_{r1}^{\Theta} - \frac{m_{CO_2} - \frac{m_{slag} \times w_{CaO}}{56} \times 44}{44 \times 3} \times \Delta H_{r2}^{\Theta}, \quad (10)$$

where Q is the heat consumption, m_i is the mass flow rate of the steelmaking slag, dilute alkali solution, and inputted CO_2 gas, C_{pi} is the specific heat capacity of the steelmaking slag, dilute alkali solution, and inputted CO_2 gas, ΔT_i is the temperature difference of the carbonation process, m_{slag} is the mass of the steelmaking slag needed for sequestrated CO_2, w_{CaO} is the mass content of CaO in the raw steelmaking slag, m_{CO_2} is the mass of CO_2 carbonated by steelmaking slag, and ΔH_{r1}^{θ} and ΔH_{r2}^{θ} are the carbonation reaction heat for calcium oxide and dicalcium silicate. Moreover, the heat consumption of the drying process is calculated as follows:

$$Q_{Dry} = \left\{ \left(\sum m_j \times c_{pj} \right) \times \Delta T_j + m_0 \times \Delta H_{evp} \right\} \times \frac{1}{\eta_{heat}}, \quad (11)$$

where m_j is the mass flow rate of the carbonated slag and entrained water, C_{pj} is the specific heat capacity of the carbonated slag and water, m_0 is the mass of the removed water, ΔH_{evp} is the heat of vapourization for water, η_{heat} is

Table 6 Power consumption of the overall process

Process power consumption	Carbonation reaction time (min)					
	30		60		120	
	$^a P_T$ (kWh)	$^b P_r$ (kWh/t)	P_T (kWh)	P_r (kWh/t)	P_T (kWh)	P_r (kWh/t)
Grinding	1674.0	267.8	1168.6	187.0	872.4	139.6
Premixing	64.6	10.3	54.4	8.7	40.5	6.5
Carbonation	64.6	10.3	83.1	13.3	103.8	16.6
Filter and washing	140	22.4	132	21.1	112	17.9
Transporter	48.3	7.7	34.9	5.6	27	4.3
Drying	681	109	495	79.2	387	61.9
Total	2672.5	427.6	1968	314.9	1542.7	246.8

$^a P_T$ refers to the total power consumption for 1 h

$^b P_r$ refers to the power consumption for every ton of sequestrated CO_2

the thermal efficiency of drier, with a selected value of 0.85, and ΔT_i is the temperature difference in the drying process, with a carbonated slag temperature after drying of 90 °C.

Based on the aforementioned calculations, the heat consumption of the integral process is listed in Table 7. As shown in Table 7, heat consumption for carbonated slag drying is considerably higher than that of the carbonation process; however, both values decrease with the increase in reaction time. Typically, considerable waste heat is released in iron and steel production process, and this heat can be effectively recovered both for steelmaking slag carbonation and for carbonated slag drying. Thus, heat consumption for the entire process will be considerably reduced.

3.2.3 Avoid CO_2 Emission Calculation

Power, heat, and reaction reagent consumption during the process will emit CO_2, whereas the utilization of carbonated product in other aspect will reduce CO_2 emission. Thus, CO_2 emission reduction of the entire process can be calculated as follows [14]:

$$
\begin{aligned}
N_{CO_2,\text{avoided}} = {} & N_{CO_2,\text{sequestered}} + m_{\text{carbonate}} \times \alpha_{\text{carbonate}} \\
& - \big(E_{\text{power}} \times \varepsilon_{\text{power}} + E_{\text{heat}} \times \varepsilon_{\text{heat}} + m_{\text{media}} \\
& \times \alpha_{\text{media}}\big),
\end{aligned}
\tag{12}
$$

where $E_{CO_2,\text{avoided}}$ is the net emission reduction of CO_2 by steelmaking, $N_{CO_2,\text{sequestration}}$ is the binding amount of CO_2 by steelmaking slag, E_{power} and E_{heat} are the power consumption and heat consumption for the whole process, respectively, ϵ_{power} and ϵ_{heat} are the equivalent CO_2 emission factors of power and heat consumption, m_{media} is the consumed reaction reagent used for CO_2 mineral sequestration with steelmaking slag, α_{media} is the equivalent CO_2 emission factor of the reaction reagent production, $m_{\text{carbonate}}$ is the quality of the carbonated product, and

$\alpha_{\text{carbonate}}$ is the equivalent CO_2 emission factor of the substitution material for carbonated product utilization.

Power mainly includes thermal power, hydrothermal power, wind power, and nuclear power. Thermal power is the only power generation process that uses coal or gas as raw material and emit large amounts of CO_2. When using advanced power generation equipment and technology, ϵ_{power} is 0.36 or 0.80 kg/kWh with less carbon content fuel for thermal power, such as advanced gas-joint power or coal-fired power generation. The calculated ϵ_{power} varies from 0.216 to 1.147 kg/kWh in China [30], and the average was 0.794 kg/kWh. Thus, ϵ_{power} is set as 0.794 kg/kWh in this work. ϵ_{heat} is also related to the required temperature for providing heat load when using conventional fossil energy as raw material for the waste heat boiler to produce steam for heating cold logistics under a certain temperature. Then, ϵ_{heat} can be calculated according to the formula of Gadalla [31] as follows:

$$
\varepsilon_{\text{heat}} = \left(\frac{Q_{\text{Fuel}}}{\text{NHV}}\right)\left(\frac{C\%}{100}\right) \times \frac{44}{12},
\tag{13}
$$

$$
Q_{\text{Fuel}} = \frac{Q_{\text{Proc}}}{\lambda_{\text{Proc}}}(h_{\text{Proc}} - 419)\frac{T_{\text{FTB}} - T_0}{T_{\text{FTB}} - T_{\text{Stack}}},
\tag{14}
$$

where C is the carbon content of fuel, NHV is the net heating value of fuel, Q_{Fuel} is the heat of fuel, Q_{Proc} is the heat load provided by fuel, T_{FTB}, T_{Stack}, and T_0 are flame temperature (1800 °C), outlet temperature of gas, and environmental temperature (25 °C), respectively, λ_{Proc} is the latent heat of saturated steam, h_{Proc} is the enthalpy value of saturated steam, and 419 is the enthalpy of deoxygenated water at 100 °C [32, 33]. The heat load in this study was provided by the waste heat boiler by using natural gas, and ϵ_{heat} is calculated as 6.028×10^{-2} kg/MJ. In this work, the mainly consumed reaction reagent is NaOH, which is produced from ionic membrane caustic soda process with sodium chloride salt as raw material. Energy, which includes 2230 kWh of electricity and 0.44 tons of steam, has to be consumed for every ton of NaOH production. Combined with the equivalent CO_2 emission factor of power and heat consumption, the α_{media} for NaOH can be calculated as 1842 kg CO_2/t NaOH. Moreover, with the active calcium in steelmaking slag possibly being completely eliminated in this process, the carbonated slag with smaller particles can be directly used as cement substitution material. Cement and cement-based material industry is known to consume a large amount of resources and emit enormous quantities of pollutants and CO_2. This industry also emits 10–20% of China's total CO_2 emission in 2009–2011 [34]. Based on material flow analysis-based potential analysis of China's cement and cement-based material industry, the average CO_2 generation for 1 t of cement production is estimated to be 873 kg [35]. Thus, the

Table 7 Heat consumption of the overall process

Process heat consumption	Carbonation reaction time (min)		
	30	60	120
Carbonation (MJ/h)	13,780	5164	112
Drying (MJ/h)	52,981	38,585	30,145
Q_T (MJ/h)[a]	66,761	43,749	30,257
Q_r (MJ/t)[b]	10,682	7000	4841

[a] Q_T refers to the total heat consumption for 1 h

[b] Q_r refers to the heat consumption for every ton of sequestrated CO_2

Table 8 CO_2 emission reduction benefits at different carbonation reaction times of the overall process

CO_2 reduction benefits	Carbonation reaction time (min)		
	30	60	120
CO_2 emission from power (kg/h)	2122	1563	1225
CO_2 emission from heat (kg/h)	4024	2637	1824
CO_2 emission from consumed NaOH (kg/h)	230	168	131
Sequestrated CO_2 (kg/h)	6250	6250	6250
Indirect avoided CO_2 emission (kg/h)	54,612	39,772	31,072
Total avoided CO_2 emission (kg/h)	54,486	41,654	34,142
Net CO_2 sequestrated by steelmaking slag (kg/t-BOFs)	968	1060	1164

CO_2 emission factor is selected as 873 kg CO_2/t carbonate in this study.

According to the above statements, the CO_2 emission reduction benefits at different carbonation reaction times of the whole process have been calculated and listed in Table 8. As shown in Table 8, with 50,000 t of CO_2 directly sequestrated by steelmaking slag per year and 6.25 tons of CO_2 sequestrated per hour, the total avoided CO_2 emission considerably decreases with the increase in reaction time. This trend mainly results from the considerable decrease in needed steelmaking slag with the extension of the reaction time. However, the net sequestrated CO_2 per ton of steelmaking slag increased with reaction time. The net avoided CO_2 emission of the entire process was 968 kg/t steelmaking slag with carbonation reaction time of 30 min and increased to 1060 kg/t steelmaking slag when the reaction time is prolonged to 60 min. The entire process exhibited efficient CO_2 emission reduction benefits when the reaction time was further prolonged to 120 min. In addition, the net avoided emission of CO_2 was 1164 kg/t steelmaking slag, which is 20% higher than that in the case of 30 min reaction time. Therefore, for CO_2 mineral sequestration with steelmaking slag, we should select the reaction time of 120 min, which results in greater superiority of CO_2 emission reduction advantages.

4 Conclusions

In this study, the enhanced CO_2 mineral sequestration with steelmaking slag in dilute alkali solution was analysed based on the experimental investigation and process evaluation. NaOH concentration is found to significantly influence calcium leaching. In comparison with pure water solution, approximately 1.8 times increase in carbonation conversion rate can be obtained at the optimum conditions of 20 g/L alkali concentration, 2 mL/g *L/S* ratio, and 70 °C reaction temperature. For the designed 50 kt/year of sequestrated CO_2 with steelmaking slag, the avoided CO_2 emission of the entire process was systematically evaluated. Carbonation reaction time significantly influenced the net CO_2 sequestration efficiency. Reaction time of 120 min would result in the avoided CO_2 emission of 1164 kg. Notably, when carbonated slag was directly used as cement substitution material, the drying process is involved in this process, which consumes considerably larger energy and results in a large amount of CO_2 emission. However, the calculated net avoided CO_2 emission for this process remains high, indicating the superiority of the benefits of reducing CO_2 emission.

References

[1] K.S. Lackner, Annu. Rev. Energy Environ. **27**, 193 (2002)

[2] K.S. Lackner, Science **300**, 1677 (2003)

[3] A. Sanna, M. Uibu, G. Caramanna, R. Kuusikand, M.M. Maroto-Valera, Chem. Soc. Rev. **43**, 8049 (2014)

[4] J. Sipilä, S. Teir, R. Zevenhoven, Åbo Akademi Rep. VT. **1**, 12 (2008)

[5] E.R. Bobicki, Q.X. Liu, Z.H. Xu, H.B. Zeng, Prog. Energy Combust. **38**, 302 (2012)

[6] W.J.J. Huijgen, G. Witkamp, R. Comans, Environ. Sci. Technol. **39**, 9676 (2005)

[7] S. Eloneva, S. Teir, J. Salminen, C.J. Fogelholm, R. Zevenhoven, Ind. Eng. Chem. Res. **47**, 7104 (2008)

[8] Y. Sun, M.S. Yao, J.P. Zhang, G. Yang, Chem. Eng. J. **173**, 437 (2011)

[9] W.J. Bao, H.Q. Li, Y. Zhang, Ind. Eng. Chem. Res. **49**, 2055 (2010)

[10] W.J. Bao, H.Q. Li, Y. Zhang, Greenh. Gases. **4**, 785 (2014)

[11] J. Yu, K. Wang, Energy Fuels **25**, 5483 (2011)

[12] S.C. Tian, J.G. Jiang, X.J. Chen, F. Yan, K.M. Li, Chem. Sustain. Chem. **6**, 2348 (2013)

[13] W.J.J. Huijgen, R.N.J. Comans, Environ. Sci. Technol. **40**, 2790 (2006)

[14] W.J.J. Huijgen, G.J. Ruijg, R.N.J. Comans, G.J. Witkamp, Ind. Eng. Chem. Res. **45**, 9184 (2006)

[15] W.J.J. Huijgen, R.N.J. Comans, G.J. Witkamp, Energy Convers. Manag. **48**, 1923 (2007)

[16] J.K. Stolaroff, G.V. Lowry, D.W. Keith, Energy Convers. Manag. **46**, 687 (2005)

[17] E.E. Chang, C.H. Chen, Y.H. Chen, S.Y. Pan, P.C. Chiang, J. Hazard. Mater. **186**, 558 (2011)

[18] S.Y. Pan, E.G. Eleazar, E.E. Chang, Y.P. Lin, H. Kim, P.C. Chiang, Appl. Energy **148**, 23 (2015)

[19] S.Y. Pan, Y.H. Chen, C.D. Chen, A.L. Shen, M. Lin, P.C. Chiang, Environ. Sci. Technol. **49**, 12380 (2015)

[20] S.Y. Pan, A.M.L. Lafuente, P.C. Chiang, Appl. Energy **170**, 269 (2016)

[21] R.M. Santos, D. François, G. Mertens, J. Elsen, T.V. Gerven, Appl. Thermal. Eng. **5**, 154 (2013)

[22] S. Eloneva, A. Said, C.J. Fogelholm, R. Zevenhoven, Appl. Energy **90**, 329 (2012)

[23] N.J. Du, L.J. Wang, Inorg. Chem. Ind. **41**, 38 (2009)

[24] H.P. Mattila, R. Zevenhoven, Chem. Sustain. Chem. **7**, 903 (2014)

[25] Y.Z. Chen, X.Q. Wang, Petro-Chem. Equip. Technol. **18**, 13 (1997)

[26] S.Q. Yuan, W.L. Cao, Fluid Eng. **20**, 35 (1999)

[27] Q. Zheng, P. Liu, Y. Fang, Mod. Mach. **6**, 87 (2010)

[28] Q.S. Ding, J. Filtr. Sep. **19**, 41 (2009)

[29] S. Datta, M.P. Henry, Y.J. Lin, A.T. Fracaro, C.S. Millard, S.W. Snyder, Ind. Eng. Chem. Res. **52**, 15177 (2013)

[30] C.M. Ma, Q.S. Ge, Adv. Clim. Change Res. **5**, 92 (2014)

[31] M.A. Gadalla, Z. Olujic, P.J. Jansens, Environ. Sci. Technol. **39**, 6860 (2005)

[32] R. Smith, O. Delaby, Chem. Eng. Res. Des. **69A**, 492 (1991)

[33] O. Delaby, R. Smith, Chem. Eng. Res. Des. **73B**, 21 (1995)

[34] J. Xu, Y. Fan, Prog. Res. Clim. Change **9**, 341 (2013)

[35] W. Wang, D. Jiang, D.J. Chen, Z.B. Chen, W.J. Zhou, B. Zhu, J. Clean. Prod. **112**, 787 (2016)